FRACTAL ANALYSIS OF BRAIN GLIAL CELLS. FRACTAL DIMENSION AND LACUNARITY

Mihai-Virgil NICHITA[1], Maria-Alexandra PAUN[2], Vladimir-Alexandru PAUN[3], Viorel-Puiu PAUN[1,4*]

Both calculated quantities in the paper, fractal dimension and lacunarity respectively, prove high precision as foreteller to classify the glial cells tissue in various brain morphologies. The importance of microglia in neurodegenerative diseases and the influence of microglia in neurological disorders have been relevated.

Keywords: fractal dimension, lacunarity, glial cells, microglia, brain diseases, Alzheimer's

1. Introduction

In human brain, not neurons, but glial cells are predominant, warns neurologist Yves Agid (Sciences et Avenir, Santé, 2017). As a rule, when we talk about our brains we refer exclusively to neurons. However, neurons are not the only ones to support, stimulate, nurture and protect the brain. There are also glial cells. In general, we are talking about the neural brain, but we need to talk about the glial brain! In the brain, glial cells, about 150 billion, are more numerous than neurons (less than 100 billion). Glial cells are of three types: microglia, immune cells that defend the brain; oligodendrogliles that accelerate electrical transmission; astrocytes, super-cells, associated indispensable neurons. Astrocytes, compared to neurons, do not have electrical activity. "Astrocytes are mute," which would explain the lesser interest in neuroscience in the twentieth century. These cells protect the neuron, harbor it and maintain contact with neurotransmitters. Also, if they do not work normally, these ignored cells are involved in the emergence of nervous system diseases, especially neurodegenerative diseases [1].

It is, therefore, an extremely important area of investigation in terms of designing new treatments that act on neurons but also on glial cells.

[1]Doctoral School, Faculty of Applied Sciences, University POLITEHNICA of Bucharest, Romania
[2]Department of Engineering, Swiss Federal Institute of Technology, (EPFL), Lausanne, Switzerland
[3]Computer Science and Systems Engineering Department Ecole Nationale Superiore de Techniques Avancées (ENSTA), ParisTech, Paris, France
[4]Physics Department, Faculty of Applied Sciences, University POLITEHNICA of Bucharest, Romania
*corresponding author: e-mail: viorel.paun@physics.pub.ro

In Fig. 1, one can see a picture of Glial cells, visually depicted from a human brain tissue.

Fig. 1. A picture of Glial cells, from the tissue of a human brain

Glial cells constitute a large fraction of the mammalian brain. Originally considered as purely non-functional glue for neurons, decades of research have highlighted the importance as well as further functions of glial cells [2]. Although many aspects of these cells are well characterized nowadays, the functions of the different glial populations in the brain under both physiological and pathological conditions remain, at least to a certain extent, unresolved.

According to a lot of research in the last decade, which neglected the importance of microglia in neurodegenerative disease, a new viewpoint in the domain on the influence of microglia in neurological disorders has been seen in the past few years since 2015. Thus, starting with 2018, which has been an exciting year, a multitude of significant contributions in this highlighted field have been achieved. In a few words, we can say that microglia is heavily involved in the occurrence of Alzheimer's disease, Parkinson's disease, Huntington's disease, Frontal Temporal dementias, ALS, Traumatic Brain Injuries, Ischaemic Strokes, Epilepsy, and other numerous neurological diseases.

In Fig. 2, a photo of human microglia cells, in contrast phase technique, is presented.

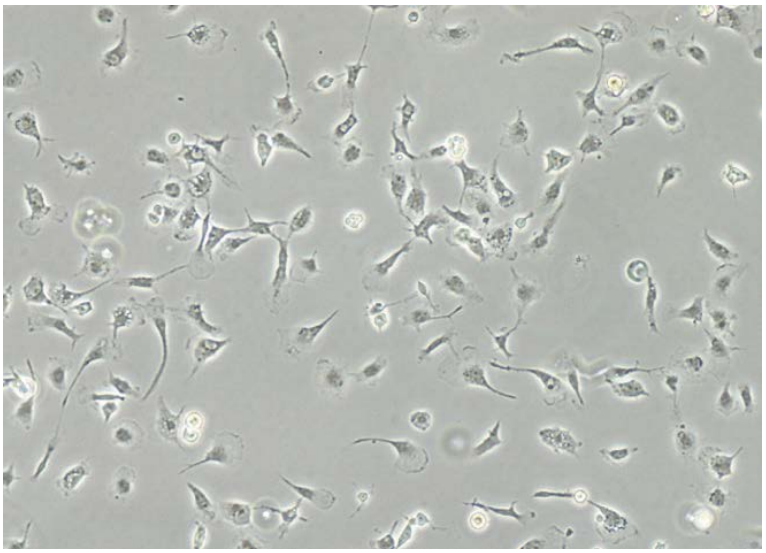

Fig. 2. A photo of human microglia cells, in contrast phase technique

Fractal analysis is a manner of measuring processes when the details of design are as important as gross morphology. It has been applied to fields as diverse as music, finance (fluctuations interpretation of foreign currency exchange rates) [3], materials technology (fractal surface analysis, fractal hydrodynamic model and fractal descriptions of the fracture parameters) [4-8], and search and rescue, in addition to topics such as signal processing (EEG/ECG), diagnostic imaging, tumor morphology, vasculature (fractal analysis in complex arterial network of pulmonary X-rays images) [9, 10] and overall brain structure, benign or malignant tissue (fractal analysis of brain tumors) [11, 12].

Before describing the metrics applied to a specific field of study we use in fractal analysis, to quantitatively characterize the fractal properties of glial cells tissue, we analyze at first the significance of the expression fractal in literature. The concept of a fractal is most often associated with geometrical objects satisfying two criteria such as self-similarity and fractional dimensionality, respectively. Self-similarity means that an object is composed of sub-units and sub-sub-units on multiple levels that (statistically) resemble the structure of the whole object [4, 5]. Mathematically, this property should hold at all scales (to be unanimously respected). However, in the real world, there are necessarily lower and upper bounds over which such self-similar behavior applies, evidently. The second criterion for a fractal object is that it has only a fractional dimension. This requirement distinguishes fractals objects from Euclidean objects, which have integer dimensions exclusively. Here we mostly refer to the fractal dimension, which will be subject to appreciable development in the following chapters.

2. Fractal analysis of Microglia cells

As with neurons, for microglia work has been published using fractal analysis to study and classify microglial morphology in neuroanatomy, pathology, and development.

One difference between the two fields of fractal analysis of neurons and of microglia is that the fractal dimension for microglia has been more clearly correlated with function.

Using box counting, it has been shown that, basically, microglia in normal, healthy brain are highly ramified with a relatively high D_B and that in response to certain stimuli such as chronic stress, they may hyper-ramify to a state with a slightly higher D_B, but when responding to fully noxious pathological events such as brain trauma, enter a cycle of deramification with concomitantly decreasing D_B, to a rounded, amoeboid form with a very low D_B, and then return through a cycle of increasing re-ramification and increasing D_B when resuming normal activity.

Different stages within the cycle are often classified using categories that describe both form and function, and the fractal dimension has been shown to objectively quantify these categories [13-15].

Much of the fractal analysis work published for microglia has used box counting based on binary silhouettes or contours, a strong point being that this methodology is robust for all of the general morphological types, branched and unbranched, facilitating comparisons. Similar to what has been seen for neurons, the fractal dimension is typically positively correlated with increasing size of the span covered by a cell but measures features in addition to size. It has been shown to delineate microglia based on other categories such as age. Also similar to what has been found for neurons, the fractal dimension for microglia objectively distinguishes cells in different pathological states (e.g. Alzheimer's). One strength of this approach is that it differentiates differences that can reflect important pathological events or other activities that are subtle or undetectable visually. For instance, the fractal dimension was useful for quantitating not only gross pathological responses but also less easily observable responses over different brain regions after transient global ischemia. This general capacity for quantifying subtleties of microglial morphology has important implications, because microglia are immune-inflammatory cells but also much more, having multiple roles in maintaining normal brain structure and function, interacting with all parts of the neuron. They are involved in pruning spines, facilitating synaptic transmission, interacting with extracellular matrix, and axonal excitability. They secrete growth factors and inflammatory mediators and play major roles in dealing with stress at all levels from sleep deprivation to subtle cognitive experience to pain modulation and severe trauma. In this respect, many roles of microglia in normal brain function and subtler dysfunction are currently being investigated suggesting the fractal

dimension of microglia will have potential application in many fields (e.g., drug monitoring, learning, stress, alcoholism and schizophrenia) [12].

Along with the fractal dimension, lacunarity and multifractal analysis have been used to classify microglial morphology. In particular, lacunarity has been used to objectively discern among very similar looking microglial morphologies within an activation category and having the same D_B (rodlike forms appear when reacting microglia fuse but could also reflect physical confines or active migration). In silico modelling has shown that the D_B is more sensitive for branching structures, but lacunarity is for particular features that are not always visually recognized such as soma size relative to process length. Multifractal analysis has shown promise for identifying microglia particularly in transitional states.

3. The box counting technique

Several methods to measure fractal dimensions and lacunarity have been used. As it is well known, the box counting technique implemented in digital image analysis software is employed with priority [13]. As expected, box counting is a way of assessing the distributions of background and non-background pixels in binary digital images representing extracted patterns from the real context of the original image [14, 15].

The differential box-counting method

Let the least and greatest grey levels be denoted by $I_{\min}$ and $I_{\max}$ respectively in the (i, j)th block. Then the total quantity of boxes essential to cover up in z direction is $n_{r\text{old}}$ and after shifting the δ positions from $n_{r\text{old}}$, $n_{r\text{new}}$ is calculated [15]. Maximum of $n_{r\text{old}}$ and $n_{r\text{new}}$ is taken as n_r. $n_r = \max(n_{r\text{old}}, n_{r\text{new}})$. $n_{r\text{old}}$ or $n_{r\text{new}}$ is calculated as follows:

$$n_r(i,j) = ceil\left(\frac{I_{max}-I_{min}}{s\prime}\right) \text{ if } I_{max} \neq I_{min} \quad (1)$$

$$n_r(i,j) = 1, \text{ otherwise} \quad (2)$$

and N_r will be calculated as

$$N_r = \sum n_r(i,j). \quad (3)$$

The fractal dimension (D_{IDBC}) is calculated with the regression plot between $\log(N)$ versus $\log(1/r)$.

Measure of Lacunarity

In overlapping or "sliding" box counting, the number of pixels per box is assessed using for each caliber, rather than a fixed grid, a single element that is systematically moved over the entire image such that the element may overlap with a previous placement at the next placement. The distribution is determined from the number of pixels per box as a function of box size or scale (ε), which is inversely

proportional to the box size. Lacunarity at a particular ε is denoted as λ_ε calculated as the squared coefficient of variation, CV, for pixel distribution:

$$\lambda_\varepsilon = (CV)^2 = \left(\frac{\sigma}{\mu}\right)^2 \quad (4)$$

where σ is the standard deviation and μ the mean of the pixels per box at ε [16, 17].

To arrive at a single number, the values for λ_ε can be summarized as the mean $\overline{\lambda}$ for the total number of calibers (E) used:

$$\overline{\lambda} = \frac{\sum \lambda_\varepsilon}{E} \ . \quad (5)$$

A normal limitation of box counting is that the pixel distribution depends on how an image is scanned [18, 19]. For some patterns more than others, placing the non-overlapping box counting grid at different orientations yields different results [20].

4. Results and Discussion

A voxel analogous to a pixel represents image data values, depicted in a 3D space. In the case of medical imaging, the position is represented on the Ox and Oy axes, while on the Oz it is represented in a gray scale the tissue resistance to the incident radiation [21. 22]. More precisely, the black color is being practically transparent to the radiation while the white color represents the reflectivity level [23, 24].

Application developed to compute lacunarity

To compute the lacunarity of a binary image, a software has been developed in MATLAB R2017a environment which assumes to cover the image of interest with a gliding window whose dimension doubles until the maximum dimension of the image of interest is reached.

The program starts by opening a window with the help of which the image of interest can be selected by introducing its name and the format in which it is stored on the computer. Then, by using the *size* function, the dimensions of the image of interest are extracted in order to define the iteration limits of the program.

During each iteration, the windows navigates the image pixel by pixel and counts the number of pixels of value 1 inside it (variable denoted by „one_pixel" in our program), as well as the squared value of this counter (variable denoted by „one_pixel2" in our program).

Further on, the lacunarity is determined with the use of the following formula:

$$Lacunarity = \frac{one\_pixel2}{one\_pixel^2} * N(n) \quad (6)$$

where N(n) represents the number of variables in the program [20].

The algorithm to compute the lacunarity has been applied subsequently to some images containing glial cells.

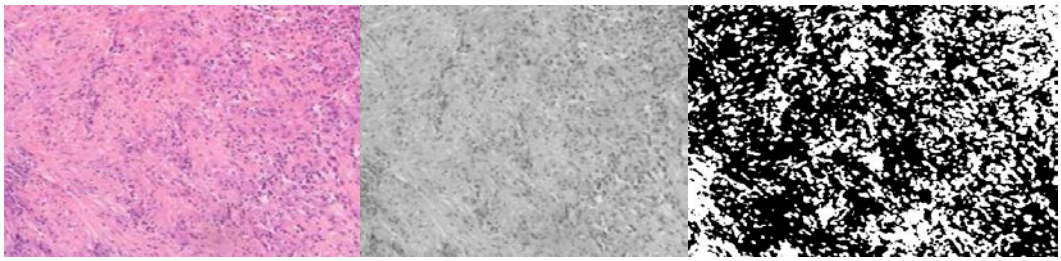

a b c

Fig. 3. a – biphasic cells; b – the shape of the image in grey-level tones; c – binary form of the image

For the image in Fig. 3c, the fractal dimension has been determined to be D_F=1.8278 ± 0.16996, the lacunarity L being given by a vector of values (1.0389, 0.9734, 0.9263, 0.8893, 0.8599, 0.8307, 0.7821, 0.5984) and an average of 0.8623 (approximated to 0.86) and Standard Deviation STDEV=0.13. Finally, the value of lacunarity is L=0.86±0.13.

In Fig. 4, the lacunarity of biphasic cells versus current number of distinct area in the inventoried tissue is represented.

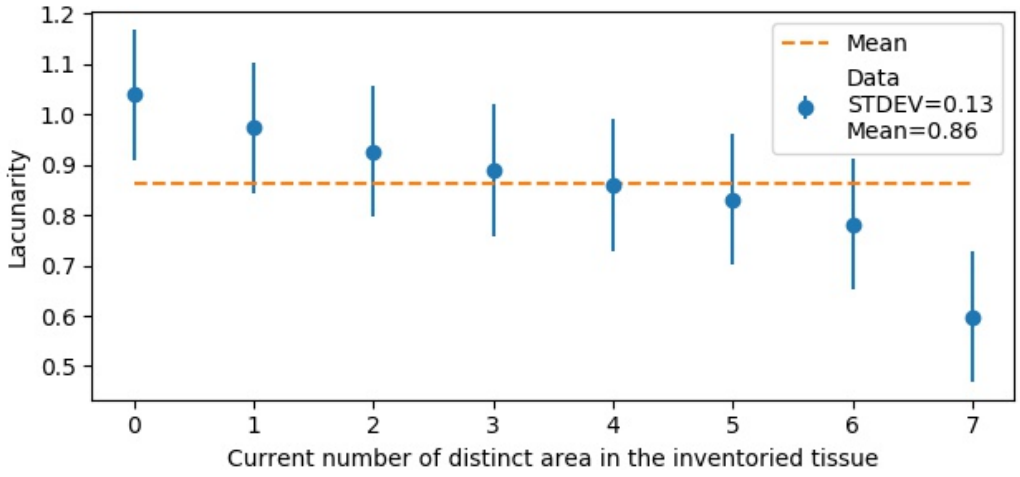

Fig. 4. The lacunarity of biphasic cells versus current number of distinct areas in the inventoried tissue

For the image in Fig. 5c, the fractal dimension has been determined to be D_F=1.8312 ± 0.17391, the lacunarity L being given by a vector of values (1.0890, 1.0069, 0.9474, 0.9011, 0.8674, 0.8369, 0.7873, 0.5948) and an average of 0.8789 (approximated to 0.88) and Standard Deviation STDEV=0.14. Finally, the value of lacunarity is L=0.88±0.14.

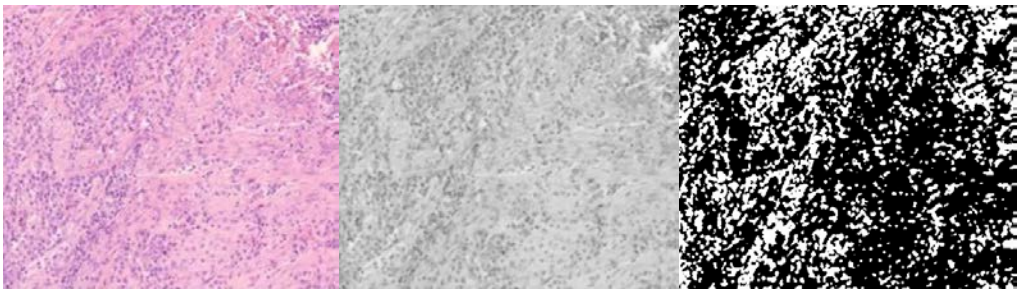

a b c

Fig. 5. a – epitheloid cells; b – the shape of the image in grey-level tones; c – binary form of the image

In Fig. 6, the lacunarity of epithelioid cells versus current number of distinct area in the inventoried tissue is represented.

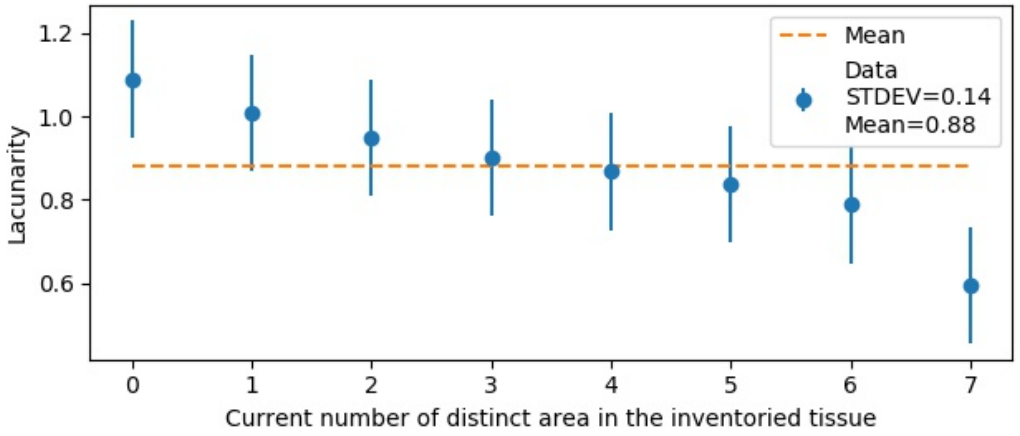

Fig. 6. The lacunarity of epithelioid cells versus current number of distinct areas in the inventoried tissue

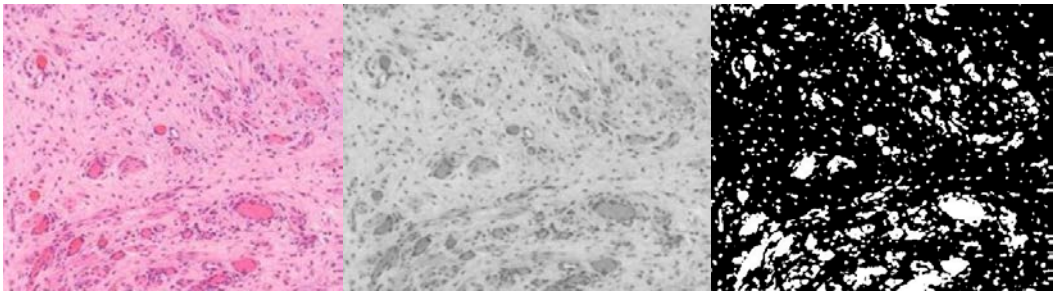

a b c

Fig. 7. a – cells of „hyperplasia" type; b – the shape of the image in grey-level tones; c – binary form of the image

For the image in Fig. 7c, the fractal dimension has been determined to be D_F=1.8285 ± 0.17076, the lacunarity *L* being given by a vector of values (1.3936, 1.2587, 1.1435, 1.0223, 0.9230, 0.8542, 0.7823, 0.5839) and an average of 0.9952

(approximated to 1.0) and Standard Deviation STDEV=0.25. Finally, the value of lacunarity is L=1.0±0.25.

In Fig. 8, the lacunarity of „hyperplasia" type cells versus current number of distinct area in the inventoried tissue is represented.

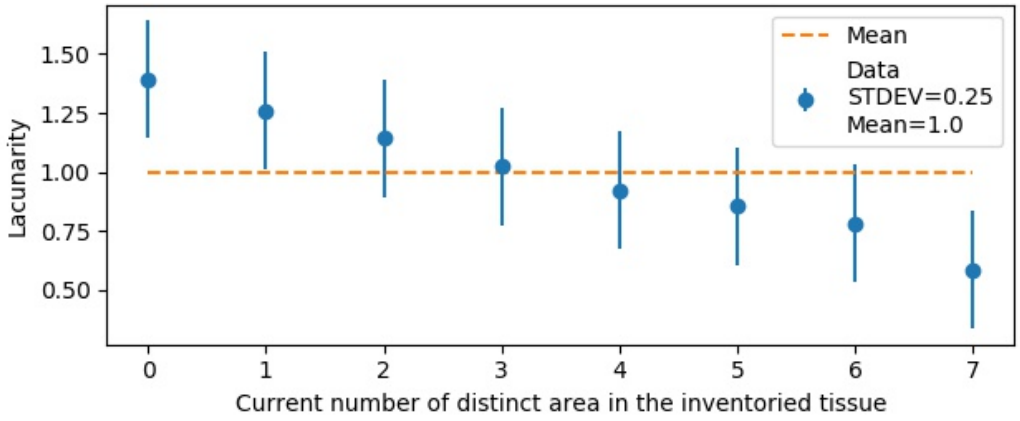

Fig. 8. The lacunarity of „hyperplasia" type cells versus current number of distinct areas in the inventoried tissue

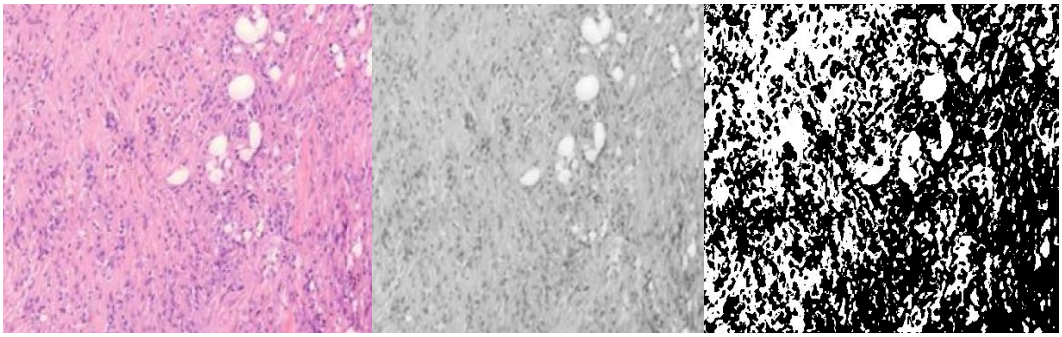

a b c

Fig. 9. a – sacramatoid cells; b – the shape of the image in grey-level tones; c – binary form of the image

For the image in Fig. 9c, the fractal dimension has been determined to be D_F=1.8285 ± 0.17076, the lacunarity L being given by a vector of values (1.5472, 1.3063, 1.1447, 1.0237, 0.9437, 0.8807, 0.8005, 0.5799) and an average of 1.0283 (approximated to 1.03) and Standard Deviation STDEV=0.28. Finally, the value of lacunarity is L=1.03±0.28.

In Fig. 10, the lacunarity of sacramatoid cells versus current number of distinct area in the inventoried tissue is represented.

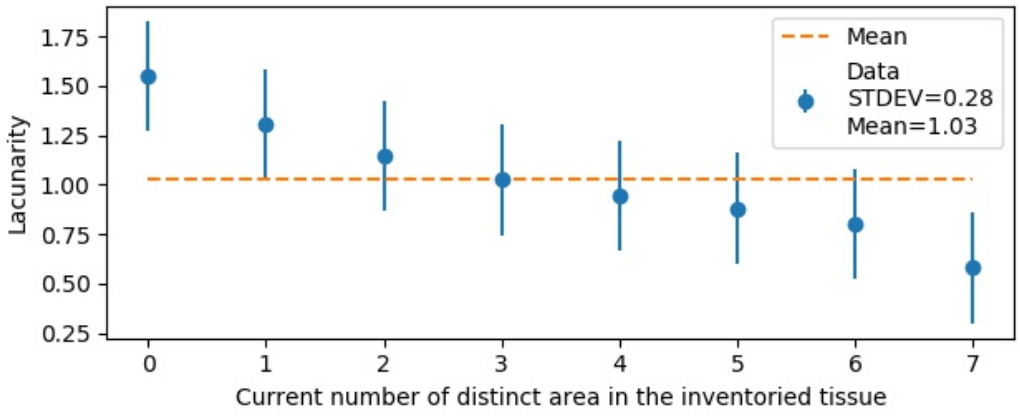

Fig. 10. The lacunarity of sacramatoid cells versus current number of distinct areas in the inventoried tissue

5. Conclusions

Whereas neurons are the critical structural and functional basis of signaling, microglia are their dynamic, constant attendants, physicians, and undertakers. Being able to quantitatively assess both of these brain cell types is vital to the overall science of understanding, monitoring, and modifying nervous system function.

It has been outlined in this paper that the D_F can be used to describe and categorize these two cell types in normal and pathological models using individual cellular branching patterns, but also other features. This work also explained that there are a variety of approaches, each with its strengths and weaknesses, making some preferred over others depending on the application. Box counting of silhouettes has particular promise for comparisons of neurons and microglia, in being able to capture features relevant to studies of both cell types in all potential forms.

In conclusion, the stage is set to draw these two fields closer, to use fractal measures of neuronal and microglial categories to investigate complex features and interactions such as signal integration, spine morphology, chemical mediators, network effects, 3D orientation, etc. Classifying tissue using this type of approach offers a perspective on connectivity and synchronicity complementing the perspective afforded by studying dendritic branching or microglial morphology alone.

Consequently, the two calculated quantities in the paper, fractal dimension D_F and lacunarity L respectively, prove high precision as foreteller of benign or malignant tumor and to classify the glial cells tissue in various brain morphologies.

The computer programs developed and detailed in this work can be entirely incorporated into a medical protocol, which can be used in detecting and monitoring of brain diseases or in other affected parts of human body.

R E F E R E N C E S

[1]. *S. Jäkel and L. Dimou,* Glial Cells and Their Function in the Adult Brain: A Journey through the History of Their Ablation, Front Cell Neurosci., vol. **11**, 2017, Article 24

[2]. *Y. Wu, L. Dissing-Olesen, B.A. MacVicar, B. Stevens,* Microglia: dynamic mediators of synapse development and plasticity, Trends Immunol., vol. 36, 2015, pp. 605–613

[3]. *S. C. Ciucu, V. P. Paun,* Financial Data Analysis Using Nonlinear Time Series Methods. Fluctuations Interpretation of Foreign Currency Exchange Rates, University Politehnica of Bucharest Scientific Bulletin -Series A-Applied Mathematics and Physics, vol. **77**, no.1, 2015, pp. 235-248

[4]. *V. P. Paun*, Fractal surface analysis of the Zircaloy-4 SEM micrographs by time series method, Central European Journal of Physics, vol. **7**, no. 2, 2009, pp. 264-269

[5]. *M. Agop, P. E. Nica, S. Gurlui, C. Focsa, V. P. Paun, M. Colotin*, Implications of an extended fractal hydrodynamic model, European Physical Journal D, vol. **56,** no.3, 2010, pp. 405-419

[6]. *D. Iordache, S. Pusca, G. Toma, V. P. Paun, A. Sterian, C. Morarescu,* Analysis of compatibility with experimental data of Fractal descriptions of the fracture parameters, Lect Notes Comput SC vol. **3980,** 2006, pp. 804-813

[7]. *V. P. Paun*, Creep model for polymeric materials, Materiale Plastice, vol. **40**, no.1, 2003, pp. 25-26

[8]. *V. P. Paun*, Relaxation model for polymeric materials in the hereditary theory of elasticity, Materiale Plastice, vol. **40**, no. 2, 2003, pp. 81-82

[9]. *P. Postolache, Z. Borsos, V. A. Paun, V. P. Paun,* New Way in Fractal Analysis of Pulmonary Medical Images, University Politehnica of Bucharest Scientific Bulletin-Series A-Applied Mathematics and Physics, vol. **80,** no.1, 2018, pp. 313-322

[10]. *M. V. Nichita, V. P, Paun,* Fractal Analysis in Complex Arterial Network of Pulmonary X-Rays Images, University Politehnica of Bucharest Scientific Bulletin -Series A-Applied Mathematics and Physics, vol. 80, no. 2, 2018, pp. 325-339

[11]. *K. M. Iftekharuddin, W. Jia, R. Marsh*, Fractal analysis of tumor in brain MR images, Machine Vision and Applications, vol. **13**, 2003, pp. 352-362

[12]. *N. Jayaraj, P. Mohanalah*, Fractal Analysis of Brain Tumors, International Journal of Innovative Research & Development, vol. **3**, no. 6, 2014, pp. 437-441

[13]. *A. L. Karperien and H. F. Jelinek*, Box-Counting Fractal Analysis: A Primer for the Clinician, Chapter 2, A. Di Ieva (ed.), The Fractal Geometry of the Brain, Springer Series in Computational Neuroscience, DOI 10.1007/978-1-4939-3995-4_2, 2016, Springer Science + Business Media New York

[14]. *S. R. Nayak, J. Mishra,* An improved method to estimate the fractal dimension of colour images, Perspectives in Science, vol. **8**, 2016, pp. 412-416

[15]. *Y. Liu, L. Chen, H. Wang, L. Jiang, Y. Zhang, J. Zhao, D. Wang, Y. Zhao, Y. Song,* An improved differential box-counting method to estimate fractal dimensions of gray-level images, J. Vis. Commun. Image Represent., vol. **25**, 2014, pp. 1102-1111

[16]. *A. Karperien, H.F. Jelinek, N.T. Milošević*, Reviewing Lacunarity Analysis and Classification of Microglia in Neuroscience, Proceedings of the 8th European Conference on Mathematical

and Theoretical Biology European Society for Mathematical and Theoretical Biology (ESMTB), 2011, MS#88

[17]. *T. G. Smith Jr., G. D. Lange, W. B. Marks*, Fractal methods and results in cellular morphology -dimensions, lacunarity and multifractals, Journal of Neuroscience Methods, vol. **69**, 1996, pp. 123-136

[18]. C*S231n*: Convolutional Neural Networks for Visual Recognition. http://cs231n.github.io/convolutional-networks/

[19]. *C. H. Dagli, Editor*, Artificial Neural Networks for Intelligent Manufacturing**,** Springer Science & Business Media, (First Edition 1994), 2012

[20]. *R. E. Plotnick, R. H. Gardner, W. W. Hargrove, K. Prestegaard, M. Perlmutter*, Lacunarity analysis: A general technique for the analysis of spatial patterns. Physical review. E, Statistical physics, plasmas, fluids, and related interdisciplinary topics **53**, 1996, pp. 5461–5468

[21]. *F. E. Lennon, G. C. Cianci, R. Kanteti, J. J. Riehm, Q. Arif, V. A. Poroyko, et al*, Unique fractal evaluation and therapeutic implications of mitochondrial morphology in malignant mesothelioma, Scientific Reports, vol. 6, 2016, Article number 24578

[22] *J. Bhattacharya, J. Edwards, A. Mamelak, E. M. Schuamn*, Ongoing hippocampal neuronal activity in human: is it noise or correlated fractal process? In: Losa GA, Merlini D, Nonnenmacher TF, Weibel ER, editors. Fractals in biology and medicine, vol IV, vol. VII. Basel: Birkhäuser Verlag Basel; 2005. p. 95–106

[23]. Key Biological Processes in the Brain. https://www.nia.nih.gov/health/what-happens-brain-alzheimers-disease

[24]. *K. J. Gorgolewski, T. Auer, R. A. Poldrack*, The brain imaging data structure, a format for organizing and describing outputs of neuroimaging experiments, Scientific Data **3**, 2016, Article number 160044